RESEARCH ARTICLE

Open Access

DESI-TQ-MS imaging for ex vivo brain biodistribution assessment: evaluation of LBT-999, a ligand of the dopamine transporter (DAT)

Laurent Galineau[1], Emmanuelle Claude[2], Zuhal Gulhan[1], Sylvie Bodard[1], Sophie Sérrière[1], Camille Dupuy[1,4], Jérémy Monteiro[1,4], Adeline Oury[1,4], Priscila Bertevello[1,4], Gabrielle Chicheri[1,4], Johnny Vercouillie[1], Lydie Nadal-Desbarats[1,4], Sylvie Chalon[1], Antoine Lefèvre[1,4] and Patrick Emond[1,3,4*]

*Correspondence:
emond@univ-tours.fr

[1] Université de Tours, INSERM, Imaging Brain & Neuropsychiatry iBraiN U1253, 37032 Tours, France
[2] Waters Corporation, Stamford Rd, Wilmslow SK9 4AX, UK
[3] Service de Médecine Nucléaire In Vitro, Hôpital Bretonneau, CHRU Tours, 37044 Tours Cedex 1, France
[4] PST Analyse Des Systèmes Biologiques - Département d'Analyse Chimique Et Métabolomique - METABOHUB, Université de Tours, Tours, France

Abstract

Background: Selection of the most promising radiotracer candidates for radiolabeling is a difficult step in the development of radiotracer pharmaceuticals, especially for the brain. Mass spectrometry (MS) is an alternative to study ex vivo the characteristics of candidates, but most MS studies are complicated by the pharmacologic doses injected and the dissection of regions to study candidate biodistribution. In this study, we tested the ability of a triple quadrupole analyzer (TQ LC–MS/MS) to quantify low concentrations of a validated precursor of a radiotracer targeting the DAT (LBT-999) in dissected regions. We also investigated its biodistribution on brain slices using MS imaging with desorption electrospray ionization (DESI) coupled to time-of-flight (TOF) vs. TQ mass analyzers.

Results: TQ LC–MS/MS enabled quantification of LBT-999 injected at sub-tracer doses in dissected striata. DESI-MS imaging (DESI-MSI) with both analyzers provided images of LBT-999 biodistribution on sagittal slices that were consistent with positron emission tomography (PET). However, the TOF analyzer only obtained biodistribution images at a high injected dose of LBT-999, while the TQ analyzer provided biodistribution images at lower injected doses of LBT-999 with a better signal-to-noise ratio. It also allowed simultaneous visualization of endogenous metabolites such as dopamine.

Conclusions: Our results show that LC-TQ MS/MS in combination with DESI-MSI can provide important information (biodistribution, specific and selective binding) that can facilitate the selection of the most promising candidates for radiolabeling and support the development of radiotracers.

Keywords: Radiotracer development, Mass spectrometry, Desorption electrospray ionization, Triple quadrupole type analyzer, LBT-999

Background

The development of new radiotracers for the central nervous system is a long and iterative multi-step process from a biomedical question to the first injection into humans (Brust et al. 2014; Van de Bittner et al. 2014). To accelerate this process, improvements have been made to rapidly progress to radiolabeling and in vivo imaging (Shaw et al. 2020). This includes focusing on the assessment of key parameters (affinity for the target, ability to cross the blood–brain barrier) to select radiotracer candidates for radiolabeling. High-throughput methods such as high performance liquid chromatography are used to obtain information on permeability, plasma protein binding and compound-membrane interactions (Shaw et al. 2020). However, the potential of radiotracer candidates based on in vitro parameters cannot always be transferred in vivo. Preclinical imaging can also be used to quickly determine whether a radiotracer candidate meets essential criteria for clinical transfer, such as crossing the blood–brain barrier, adequate biodistribution and kinetics, and selective and specific binding to the molecular target. Though, radiolabeling is still limited to laboratories with special infrastructure and knowledge in radiochemistry. Thus, there is a need for new methods that can provide important information to select the most promising radiotracer candidates prior to radiolabeling.

In this context, mass spectrometry (MS) has been proposed to achieve this goal (Barth et Need 2014). MS coupled to high performance liquid chromatography (LC–MS) can be used to quantify a candidate injected into an animal in dissected of regions of interest (Chernet et al. 2005; Barth et al. 2006; Ma et al. 2009, 2010; Barth et Need 2014; Xiao et al. 2018; Gilardoni et al. 2022). However, most LC–MS studies have injected pharmacological doses of tracers (Chernet et al. 2005; Barth et al. 2006; Need et al. 2007; Chen et al. 2015; Xiao et al. 2018) and are limited to the dissected regions, potentially diluting the specific binding of the tracer by not accounting for the heterogeneity of the target's expression within the region (Barth et Need 2014). This can be partially overcome by MS imaging (MSI) on brain slices with desorption electrospray ionization (DESI-MSI) or matrix assisted laser desorption/ionization (MALDI-MSI). MALDI and DESI-MS imaging are based on different ionization principles. MALDI MS imaging requires a matrix coating and vacuum conditions, while DESI-MS imaging involves spraying the sample with an electronically charged solution under ambient conditions. Each technique has its own advantages and limitations. DESI-MS imaging is an attractive method as it requires little pretreatment, can analyze samples faster and offers the possibility to perform multiple MS or other analyzes (immunohistochemistry) on the same sample (Wu et al. 2010; Eberlin et al. 2011; Barre et al. 2017; Porta Siegel et al. 2018; He et al. 2022; Djambazova et al. 2023).

In this proof-of-concept study, we aimed to demonstrate that LC–MS in combination with DESI-MSI are suitable to support radiotracer candidate selection prior to radiolabeling based on the increased sensitivity and resolution of MS, using the example of LBT-999 ((E)-N-(4-fluorobut-2-enyl)2β-carbomethoxy-3β-(4'-tolyl)nortropane), the cold analogue of 18F-LBT-999, which is a radiotracer of DAT developed and validated in our laboratory. We performed biodistribution experiments in rats injected with LBT-999 at different concentrations and used a triple quadrupole (TQ)

analyzer to detect LBT-999 in dissected tissues. We also compared two types of analyzers (TOF vs. TQ) for the detection of LBT-999 in sagittal brain slices.

Methods

Animals

Six adult male Wistar rats (Janvier, Le-Genest-Saint-Isle, France) arrived at the animal facility and were housed in the same cage for one week prior to use under constant humidity and temperature conditions with a 12:12 light:dark cycle (lights off at 7:00 am) and ad libitum access to food and water. All animal experiments were conducted in accordance with the requirements of the European Community Council Directive 2010/63/EU for the care of laboratory animals and approved by our local ethics committee (comité d'éthique en experimentation animale Val de Loire #4208-2016022218004689).

Biodistribution experiments on dissected tissues

Under anesthesia (Vetflurane 4% for induction, 2% for maintenance; Virbac, Centravet, France), two rats were injected with different doses of LBT-999 into the penile vein (0.02 mg/kg and 0.0002 mg/kg, corresponding to a 50-fold increase and half the tracer dose), while a third rat underwent the same protocol without any LBT-999 injection and served for MS calibration. Sixty minutes after injection, each rat was sacrificed by decapitation and its brain carefully removed on ice. Regions of interest with different DAT densities (high densities in the striatum versus low densities in the frontal cortex, hippocampus and cerebellum; Ciliax et al. 1995; Galineau et al. 2004; Sérrière et al. 2014; Flace et al. 2021) were dissected and stored at −80 °C until use.

Subsequently, each brain region was freeze-dried and homogenized to powder. A quantity of 3 mg dry was weighed before extraction. For the calibrator and control samples, the brain of the rat that had not been injected with LBT-999 was freeze-dried, and 3 mg was used as a surrogate matrix. Calibrators, controls and samples were prepared as described in Table 1.

Table 1 Composition of calibrators, controls and samples

| Calibrators/ Controls/ Samples	Volume of spiking solution (µL)[a]	Volume of internal standard solution (µL)[b]	Volume of extraction solution (µL)[c]	Final concentration of LBT-999 (pg/mL)
Cal 1	100	100	300	3.75
Cal 2				12.50
Cal 3				25
Cal 4				125
Cal 5				375
Cal 6				1250
Cal 7				2500
Low QC				100
Medium QC				1000
High QC				2000
Sample	100[d]			–

(a) LBT-999 solutions in water, (b) Cocaine solution (2.5 ng/mL) in water, (c) MeOH/Water (8:2), (d) Water solution without LBT-999. Low, medium and high QC refer on the LBT-999 concentration in the QC samples based on the calibration curve

After addition of all solutions, planar shaking at room temperature for 30 min and centrifugation at 15,000 g at 4 °C for 10 min were performed. The levels of LBT-999 were measured by HPLC coupled to a TQ-XS MS spectrometer (Waters Corporation, Wilmslow, UK). Five microliters of the supernatant were injected into the system. Chromatography was performed using a Phenomenex Kinetex 1.7 μm XB-C18 (150 mm × 2.10 mm) and 100 Å HPLC column maintained at 55 °C. The solvent system comprised mobile phase A [0.5% (vol./vol.) formic acid in water] and mobile phase B [0.5% (vol./vol.) formic acid in methanol] at a flow rate of 0.4 mL/min. Multiple Reaction Monitoring (MRM) analyses were performed in positive electrospray ionisation mode (ESI+) with a cone voltage of 20 V, a collision energy of 30 for LBT-999 and 25 eV for cocaine (methyl (1R,2R,3S,5S)-3-benzoyloxy-8-methyl-8-azabicyclo[3.2.1]octane-2-carboxylate), which was used as an internal standard, and a dwell time of 173 ms. The MRM transitions were 332.1 > 154.1 for LBT-999 (Tr = 7.37 min) and 304.1 > 182.1 for cocaine (Tr = 6.14 min). The acquired data were processed using Masslynx 4.2® software (Waters Corporation, Wilmslow, UK) by integrating selected product ion chromatographic peak areas. The calibration curve was generated by calculating the intensity ratio between LBT-999 and cocaine and used to calculate LBT-999 concentrations in the quality control (QC) and brain samples. The typical chromatogram and calibration curve are shown in Fig. 1.

DESI-MSI

Two rats received intravenous (penile vein) LBT-999 at doses of 2 and 0.02 mg/kg, and a third rat was pretreated with a high concentration of GBR 12909 (1-(2-bis(4-fluorophenyl)methoxy)ethyl)-4-(3-phenylpropyl)piperazine hydrochloride), a well-described DAT antagonist (Ki = 1 nM; 12.5 mg/kg, i.p.; Sigma-Aldrich, Saint-Quentin-Fallavier, France) 15 min before injection of LBT-999 at 0.02 mg/kg (i.v.). Each rat was killed by decapitation 60 min after LBT-999 injection and its brain was carefully removed on ice. Half of the brain was directly frozen at −80 °C for sagittal sectioning, and the other half was used to dissect the same regions as previously described. The dissected regions were stored at −80 °C until use. Twenty micrometer thick sagittal brain sections were cut with a cryostat (Leica, France) 1.5–2.5 mm from the bregma in the medio-lateral axis to include regions containing the dopaminergic neurons and the projection areas in the same section. The brain sections were stored at −80 °C until use.

Initial DESI-MSI experiments were performed in full-scan MS and MS/MS positive mode using a 2D Omni spray stage (Prosolia, Indianapolis, US) coupled with a Xevo G2-XS QTof mass spectrometer (Waters Corporation, Wilmslow, UK). The Prosolia DESI source was also connected to Xevo TQ-XS mass spectrometers (Waters Corporation, Wilmslow, UK) to perform DESI-MSI-MRM experiments. The first generation Waters DESI sprayer was used and the MRM transition for LBT-999 was 332.1 > 154.1. Further experiments were performed using a DESI XS source (Waters Corporation, Wilmslow, UK) containing the High-Performance DESI sprayer mounted on a Xevo TQ-XS mass spectrometer (Waters Corporation, Wilmslow, UK), with data acquired in MRM mode. For these experiments, MRM transitions were defined for LBT-999 (332.1 > 154.1), but also for dopamine, the endogenous ligand of DAT (154.1 > 137.1), as well as for two lipids from the
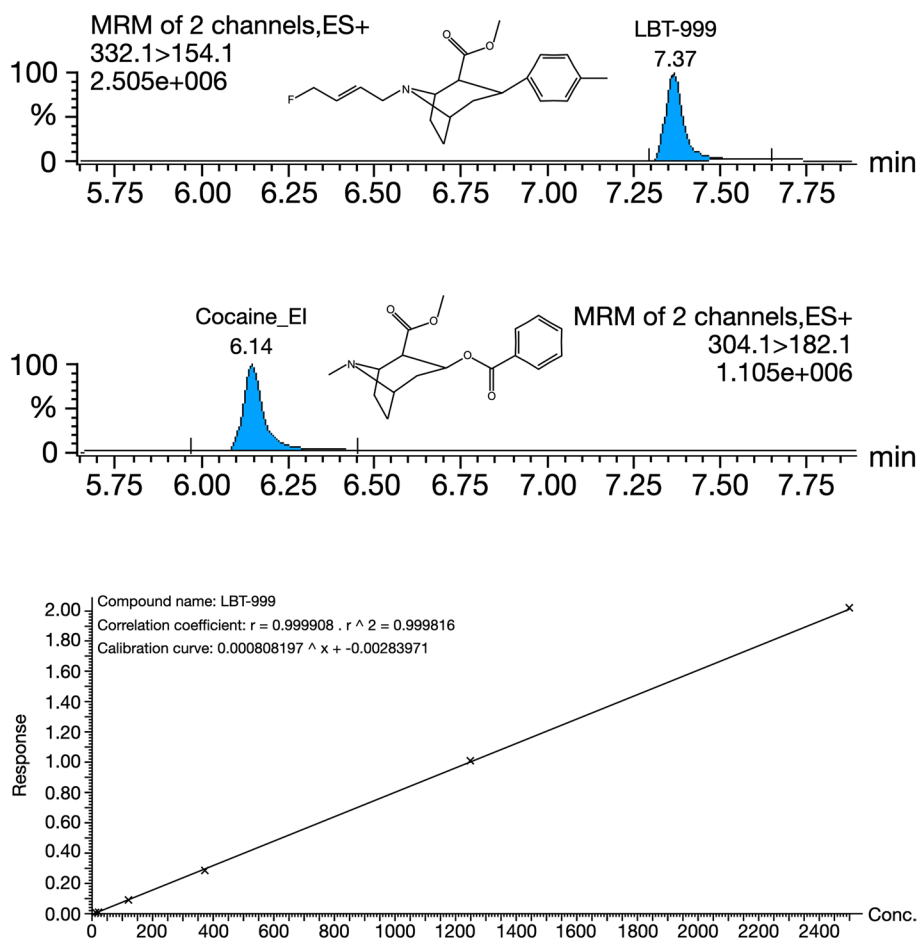
Fig. 1 LBT-999 quantification using HPLC-TQ-MS. Cocaine is used as an internal standard for the calibration and the determination of LBT-999 in brain tissues

phosphatidylcholine (PC) group, which are the most abundant lipids in the brain (O'Brien and Sampson 1965) and were used to visualise the entire brain anatomy (786.6 > 184 for protonated PC [36:2] and 820.55 > 163 for potassiated PC [36:4]). In all experiments, DESI spray solvent (95:5 methanol/water) was delivered at a flow rate of 2 μL/min. The conditions of the first generation DESI sprayer were a capillary voltage of 4.6 kV, nebulizing gas at 5.0 bar, a pixel size of 100 μm and solvent delivery with a Harvard syringe pump, while the conditions of the high-performance device were a capillary voltage of 0.6 kV, nebulizing gas at 0.6 bar, a pixel size of 50 μm and solvent delivery with a Nanoflow pump acquit UPLC. High-Definition Imaging (HDI) 1.7 (Waters Corporation, Wilmslow, UK) with the DESI Method Editor was used to set up experiments, process and visualize the imaging data. Data were acquired using MassLynx software version 4.2 (Waters Corporation, Wilmslow, UK). Relative quantification of dopamine intensities in each sagittal slice was performed by dividing the average intensities of 10 regions (10 circles of 80 pixels) drawn in the middle part of the striatum in the mediodorsal axis for LBT-999 and dopamine from those for lipids.

Results

LBT-999 detection in dissected regions

LBT-999 was detected by TQ LC–MS/MS in striatal samples from rats injected with the unlabeled tracer at concentrations of 0.02 and 0.0002 mg/kg (Table 2). The percentage of injected doses that were quantified ranged from 1.7 to 2.5% for the 0.02 and 0.0002 mg/kg doses, respectively. In contrast, LBT-999 was detected in extra-striatal regions only at the injected dose of 0.02 mg/kg, with the percentage of the injected dose ranging from 0.08 to 0.10% in the cortex, hippocampus and cerebellum (Table 2). The average percentage of injected doses derived from PET studies using 18F-LBT-999 in the striatum was $2.17 \pm 0.42\%$ (Additional Table 1 from data previously published in Sérrière et al. 2014).

LBT-999 biodistribution using DESI-MSI

Using DESI-MSI with a TOF analyzer in two different modes, we detected LBT-999 injected at a dose of 2 mg/kg in sagittal brain slices (Fig. 2). The obtained images showed a marked striatal accumulation of LBT-999 and a signal-to-noise ratio of 1:3–1:8 in the full-scan MSI and targeted MS/MS modes, respectively (Fig. 2). Under our conditions, LBT-999 injected at a concentration of 0.02 mg/kg was not detected in the sagittal brain slices regardless of the imaging mode. In contrast, DESI-MSI with a TQ-type analyzer in MRM acquisition mode provided biodistribution images of sagittal brain slices from rats for both 2 and 0.02 mg/kg injected LBT-999 with a marked striatal accumulation and a signal-to-noise ratio of 1:50 and 1:5, respectively (Fig. 2). The improvement in spatial resolution from 100 to 50 µm enabled the detection of LBT-999 in the substantia nigra / ventral tegmental area (SN/VTA) dopaminergic cell bodies for 0.02 mg/kg injected into the animal, whereas it was indistinguishable from noise when 2 mg/kg was injected (Fig. 3). Colocalization between LBT-999 and dopamine was apparent at the striatal level, but also at the SN/VTA level (Fig. 4). A blocking experiment in which a rat was injected with GBR12909 as a DAT antagonist prevented any binding of LBT-999 injected at a dose of 0.02 mg/kg and resulted in a 2.2-fold increase in normalized intensities of striatal dopamine (Fig. 4).

Table 2 Cerebral biodistribution in rats after a 0.02 or 0.0002 mg/kg injection of LBT-999

Rat weight (g)	Injected dose of LBT-999 (mg/kg)	Brain area	Weight of the dissected area (mg)	LBT-999 concentration (ng/g tissue)	% of injected dose/g tissue
292	0.02	Striatum	40.2	98.3	1.69
		Cortex	179.1	5.8	0.10
		Hippocampus	73.1	4.6	0.08
		Cerebellum	46.9	4.7	0.08
366	0.0002	Striatum	36.3	1.8	2.49
		Cortex	181.7	ND	ND
		Hippocampus	69.9	ND	ND
		Cerebellum	56.0	ND	ND

Percentages of injected dose/g of tissues were determined 60 min after injection
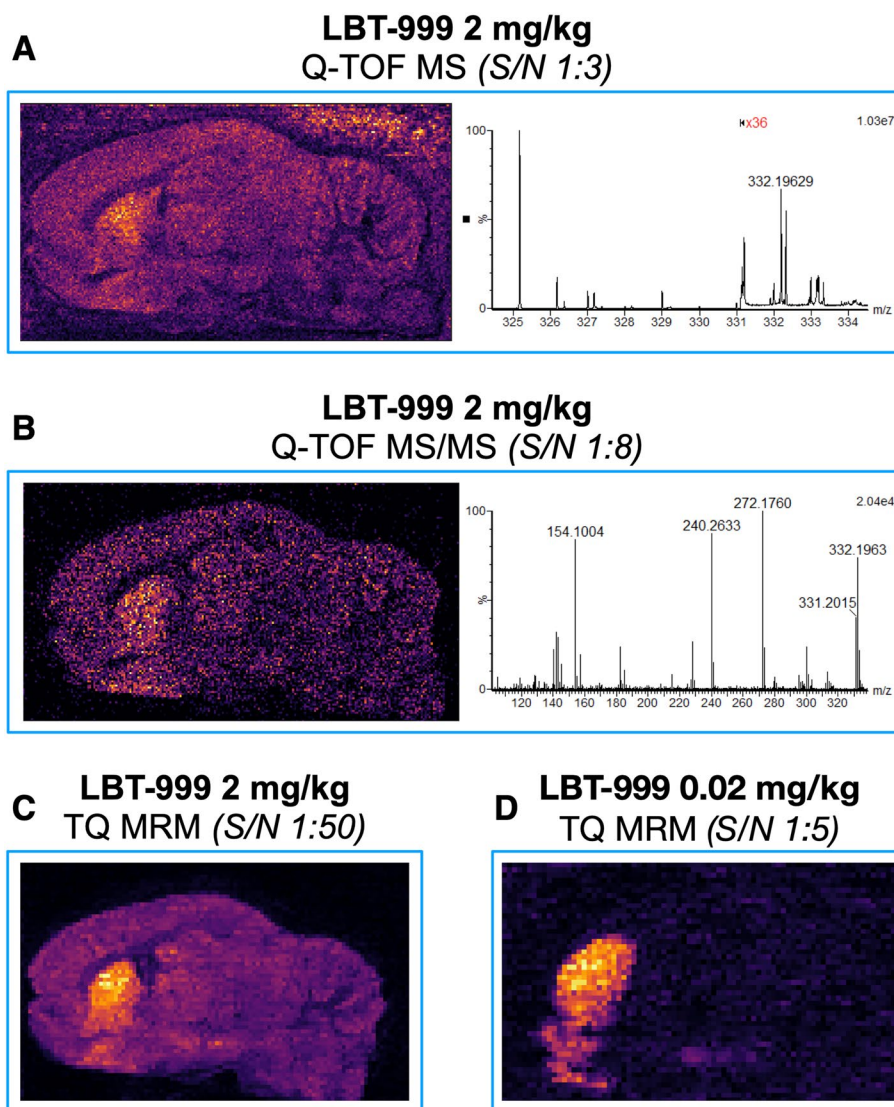
Fig. 2 Comparison of LBT-999 accumulation in rat brain using Q-TOF/TQ and DESI. **A** and **B** images of brain sagittal slices and spectra obtained in MS mode (m/z 332.1) and MS/MS mode (m/z 154.1), respectively using a Xevo G2-XS QTOF mass spectrometer from a rat injected with 2 mg/kg of LBT-999. **C** and **D** images of brain sagittal slices obtained using a Xevo TQ-XS MS spectrometer in MRM mode (332.1 > 154.1) from rats injected with LBT-999 at 2 and 0.02 mg/kg, respectively. Spatial resolution 100 μm

Discussion

This proof-of-concept study showed that LC–MS/MS with a TQ analyzer could detect LBT-999 injected in subtracer doses in dissected rat striatal tissue. We also showed that this type of analyzer with DESI-MSI provided biodistribution images of LBT-999 on rat sagittal slices consistent with PET imaging of the biodistribution of 18F-LBT-999 (Sérrière et al. 2014), and also showed its colocalization with dopamine and prevention of its brain accumulation in blocking experiments.

The first approach using MS to detect tracer candidates in dissected tissue was proposed several years ago, but was confounded by the high doses of cold radiotracer analogues that had to be injected into the animals to detect the compound in the brain (Chernet et al. 2005;
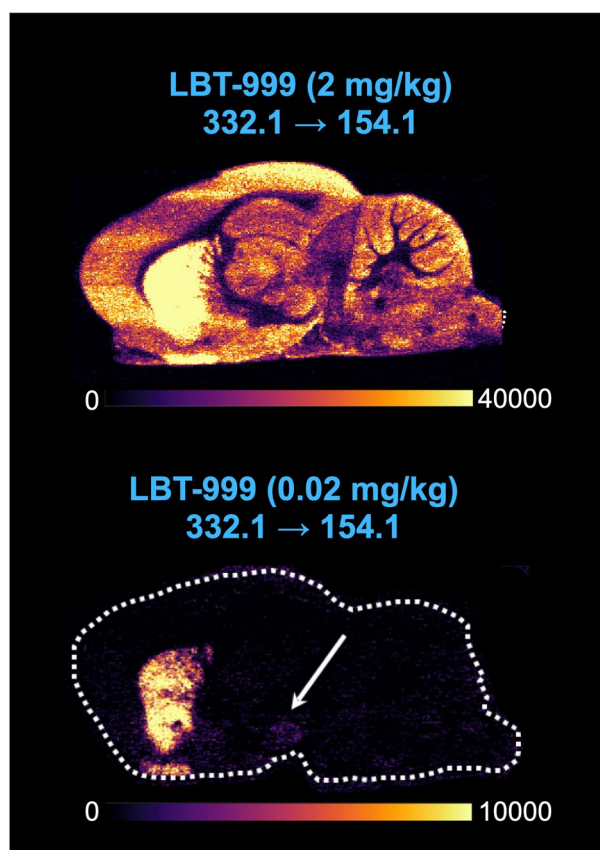
Fig. 3 LBT-999 accumulation in a rat brain sagittal section using TQ and DESI at moderate resolution. Sagittal images of LBT-999 accumulation in the rat brain using a Xevo TQ-XS MS spectrometer in MRM mode (332.1 > 154.1) of sagittal slice from rats injected with LBT-999 at 2 and 0.02 mg/kg. Arrow showing the accumulation in the SN/VTA. Spatial resolution 50μm
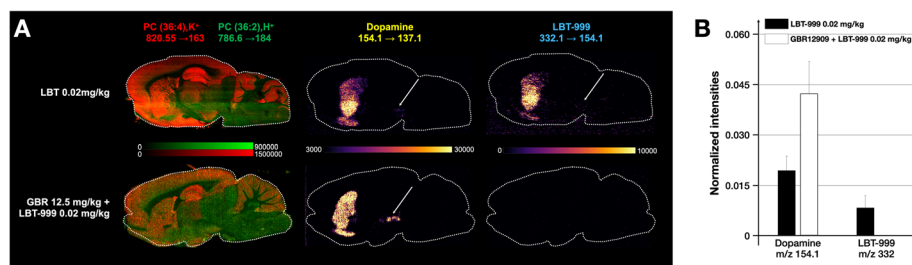
Fig. 4 DESI TQ MS to image LBT-999 and dopamine accumulations. **a.** From left to right, ion images of two lipids (potassiated PC(36:4) and protonated PC (36:2)), dopamine (154.1 > 137.1), and LBT-999 (332.1 > 154.1) acquired using the DESI TQ-XS mass spectrometer of sagittal brain sections from rats injected with LBT-999 at the dose of 0.02 mg/kg (upper panel), and a DAT antagonist (GBR12909, 12.5 mg/kg) 15 min before 0.02 mg/kg LBT-999 injection (lower panel). Arrows pointing the SN/VTA. Spatial resolution 50 μm. **b.** Relative quantification of dopamine and LBT-999 intensities relative to the signals from the lipids measured in the striatum in a rat injected with LBT-999 (0.02 mg/kg), and in a rat pre-treated with GBR12909 (12.5 mg/kg) 15 min before LBT-999 injection (0.02 mg/kg)

Barth et al. 2006; Need et al. 2007; Ma et al. 2009). With the technological advances in MS instrumentation, a recent study has shown that this approach using a TQ analyzer enables the detection of tracer doses of unlabeled tracers (Xiao et al. 2018). Using TQ LC–MS/MS,

we observed a profile of LBT-999 brain accumulation in the striatum versus extra-striatal areas that was consistent with what we had previously described using biodistribution/PET imaging studies and 18F-LBT-999 (Sérrière et al. 2014), where LBT-999 was injected at half the tracer dose. Furthermore, the striatal percentages of the injected dose were similar to those we had determined in PET experiments with 18F-LBT-999 (additional Table 1; Sérrière et al. 2014). This underlines that TQ LC–MS/MS can detect very low concentrations of cold analogues of radiotracer candidates in dissected tissue and that it can be used to select the most promising radiotracer candidates for radiolabeling. This opens up the possibility of performing biodistribution studies with multiple tracers of a target injected into an animal without occupying the target to an extent that leads to functional changes.

However, it is also important to obtain information about the binding of a compound without having to dissect the areas of interest. To this end, DESI-MSI provides a way to visualize the entire binding distribution of the molecule ex vivo in a single analysis. In several studies, DESI-MSI has already been used for ex vivo biodistribution of molecules in different contexts and has the advantage of minimal sample preparation compared to MALDI-MSI (Walch et al. 2008; Wu et al. 2010; Eberlin et al. 2011; Liu et al. 2014; Fernandes et al. 2016; Shariatgorji et al. 2016).

We first showed that TQ analyzers are better to detect unlabeled LBT-999 in sagittal brain slices compared to TOF analyzers, allowing lower amounts of unlabeled tracer to be injected into the animal and resulting in images with a higher signal-to-noise ratio. While there was an increase in signal-to-noise ratio when using the targeted MS/MS mode compared to the full-scan MS mode with the TOF analyzer, the increase was dramatically greater when comparing the TQ to the TOF analyzers, and only the TQ DESI-MSI provided images of LBT-999 brain accumulation at a low dose of tracer injected into the animal. Even though the TOF analyzers allow non-targeted studies of metabolism and provide a large amount of information, the detection of low concentrations of ligands/molecules is limited by their sensitivity, whereas the TQ analyzers are generally more sensitive. One limitation is that TQ DESI-MSI cannot yet provide images of biodistribution of candidates injected with tracer doses. However, a recent study showed comparable biodistributions of a 5HT2A/2C agonist with DESI-MSI, autoradiography and PET imaging (Jacobsen et al. 2021) as we have shown for LBT-999. In addition, the ability to detect endogenous molecules that bind to the target of interest in the same section makes DESI-MSI a unique tool for preclinical characterization of new radiotracer candidates. The blocking experiment performed with GBR12909 provided images of the lack of binding of LBT-999 in the brain slice together with the detection of increased dopamine intensities compared to control conditions, which may reflect the pharmacological effect of pretreatment (Westerink et al. 1987). DESI-MSI can thus provide information on the accumulation and biodistribution of radiotracer candidates in the brain under different conditions to assess their selective and specific binding, but also provide an image of the metabolic environment in the regions of interest.

Conclusions

These results demonstrated that LC–MS/MS experiments could detect cerebral biodistribution of LBT-999 for injected concentrations lower than the tracer doses and that the biodistribution was consistent with the biodistribution data obtained for the

radiolabeled analogue. Furthermore, we have shown that TQ analyzers can be used for both ex vivo biodistribution and DESI-MSI. Thus, the same analyzer can be used for biodistribution experiments with tracer doses, can perform MSI on sections with a spatial resolution better than autoradiography, and can image radiotracer candidates, endogenous ligands, and their metabolic environment simultaneously in the same section. Taken together, the incorporation of TQ LC–MS/MS and DESI-MSI into the radiotracer development workflow can further facilitate and improve the screening of candidates based on their ability to cross the blood–brain barrier and accumulate regio-selectively based on their target expression. This can be crucial for the development strategy of new molecules by reducing time-consuming and expensive radiolabeling.

Abbreviations

Cal	Calibrators
DAT	Dopamine transporter
DESI	Desorption electrospray ionization
DESI-MSI	Desorption electrospray ionization mass spectrometry imaging
ESI+	Positive electrospray ionization mode
HDI	High-definition imaging
HPLC	High-performance liquid chromatography
I.p.	Intraperitoneal
I.v.	Intravenous
LC–MS	Mass spectrometry coupled to high performance liquid chromatography
MALDI-MSI	Matrix assisted laser desorption/ionization mass spectrometry imaging
MS	Mass spectrometry
MSI	Mass spectrometry imaging
MRM	Multiple reaction monitoring
PC	Phosphatidylcholines
PET	Positron emission tomography
QC	Quality control
SN/VTA	Substantia nigra / ventral tegmental area
TOF	Time-of-flight analyzer
TQ	Triple quadrupole analyzer
UPLC	Ultra performance liquid chromatography

Supplementary Information

The online version contains supplementary material available at https://doi.org/10.1186/s41181-024-00289-5.

> Supplementary Material.

Availability of data and materials
The datasets generated during and/or analysed during the current study and not found in the supplementary information are available from the corresponding author on reasonable request.

Declarations

Ethics approval and consent to participate
All animal experiments were conducted in accordance with the requirements of the European Community Council Directive 2010/63/EU for the care of laboratory animals and approved by our local ethics committee (comité d'éthique en experimentation animale Val de Loire #4208-2016022218004689). All animals were purchased from Janvier Labs (Le-Genest-Saint-Isle, France) which is the ISO 9001 certified ensuring the highest standards of veterinary care.

Consent for publication
Not applicable to this study.

Competing interests
The authors have no relevant financial or non-financial interests to disclose.

References
Barre FPY, Heeren RMA, Potocnik NO. Mass spectrometry imaging in nanomedicine: unraveling the potential of msi for the detection of nanoparticles in neuroscience. CPD. 2017;23(13):1974–84. https://doi.org/10.2174/1381612823 666170111112550.

Barth V, Need A. Identifying novel radiotracers for PET Imaging Of The Brain: Application of LC-MS/MS to tracer identification. ACS Chem Neurosci. 2014;5(12):1148–53. https://doi.org/10.1021/cn500072r.

Barth VN, Chernet E, Martin LJ, Need AB, Rash KS, Morin M, et al. Comparison of rat dopamine D2 receptor occupancy for a series of antipsychotic drugs measured using radiolabeled or nonlabeled raclopride tracer. Life Sci. 2006;78(26):3007–12. https://doi.org/10.1016/j.lfs.2005.11.031.

Brust P, van den Hoff J, Steinbach J. Development of 18F-labeled radiotracers for neuroreceptor imaging with positron emission tomography. Neurosci Bull. 2014;30(5):777–811. https://doi.org/10.1007/s12264-014-1460-6.

Chen H, Lester-Zeiner D, Shi J, Miller S, Glaus C, Hu E, et al. AMG 580: a novel small molecule phosphodiesterase 10A (PDE10A) positron emission tomography tracer. J Pharmacol Exp Ther. 2015;352(2):327–37. https://doi.org/10.1124/jpet.114.220517.

Chernet E, Martin LJ, Li D, Need AB, Barth VN, Rash KS, et al. Use of LC/MS to assess brain tracer distribution in preclinical, in vivo receptor occupancy studies: dopamine D2, serotonin 2A and NK-1 receptors as examples. Life Sci. 2005;78(4):340–6. https://doi.org/10.1016/j.lfs.2005.04.075.

Ciliax J, Demchyshyn L, Pristupa B, Niznik B, Levey I. The dopamine transporter: Immunochemical characterization and localization in Brain. J Neurosci. 1995;15(3):1714–23. https://doi.org/10.1523/JNEUROSCI.15-03-01714.1995.

Djambazova KV, Van Ardenne JM, Spraggins JM. Advances in imaging mass spectrometry for biomedical and clinical research. TrAC Trends Anal Chem. 2023;169: 117344. https://doi.org/10.1016/j.trac.2023.117344.

Eberlin LS, Ferreira CR, Dill AL, Ifa DR. Cooks RG (2011) Desorption electrospray ionization mass spectrometry for lipid characterization and biological tissue imaging. Biochim Et Biophys Acta (BBA) Molecular Cell Biol Lipids. 1811;11:946–60. https://doi.org/10.1016/j.bbalip.2011.05.006.

Fernandes AMAP, Vendramini PH, Galaverna R, Schwab NV, Alberici LC, Augusti R, et al. Direct visualization of neurotransmitters in Rat brain slices by desorption electrospray ionization mass spectrometry imaging (DESI - MS). J Am Soc Mass Spectrom. 2016;27(12):1944–51. https://doi.org/10.1007/s13361-016-1475-0.

Flace P, Livrea P, Basile GA, Galletta D, Bizzoca A, Gennarini G, et al. The cerebellar dopaminergic system. Front Syst Neurosci. 2021;15: 650614. https://doi.org/10.3389/fnsys.2021.650614.

Galineau L, Kodas E, Guilloteau D, Vilar MP, Chalon S. Ontogeny of the dopamine and serotonin transporters in the rat brain: an autoradiographic study. Neurosci Lett. 2004;363(3):266–71. https://doi.org/10.1016/j.neulet.2004.04.007.

Gilardoni E, Zana A, Galbiati A, Sturm T, Millul J, Cazzamalli S, et al. A mass spectrometry-based method for the determination of in vivo biodistribution of tumor targeting small molecule-metal conjugates. Pharmacol Toxicol. 2022;94(30):10715–21. https://doi.org/10.1021/acs.analchem.2c01104.

He MJ, Pu W, Wang X, Zhang W, Tang D, Dai Y. Comparing DESI-MSI and MALDI-MSI mediated spatial metabolomics and their applications in cancer studies. Front Oncol. 2022;12: 891018. https://doi.org/10.3389/fonc.2022.891018.

Jacobsen SC, Speth NR, Xiong M, Herth MM, Kristensen JL, Palner M, et al. Desorption electrospray ionization mass spectrometry imaging of cimbi-36, a 5-HT2A receptor agonist, with direct comparison to autoradiography and positron emission tomography. Mol Imaging Biol. 2021;23(5):676–85. https://doi.org/10.1007/s11307-021-01592-2.

Liu J, Gingras J, Ganley KP, Vismeh R, Teffera Y, Zhao Z. Whole-body tissue distribution study of drugs in neonate mice using desorption electrospray ionization mass spectrometry imaging: Whole-body tissue distribution study by DESI-MSI. Rapid Commun Mass Spectrom. 2014;28(2):185–90. https://doi.org/10.1002/rcm.6775.

Ma Y, Lang L, Reyes L, Tokugawa J, Jagoda EM, Kiesewetter DO. Application of highly sensitive UPLC–MS to determine biodistribution at tracer doses: validation with the 5-HT1A ligand [18F]FPWAY. Nucl Med Biol. 2009;36(4):389–93. https://doi.org/10.1016/j.nucmedbio.2009.01.002.

Ma YO, Kiesewetter D, Lang L, Gu D, Chen X. Applications of LC-MS in PET radioligand development and metabolic elucidation. CDM. 2010;11(6):483–93. https://doi.org/10.2174/138920010791636167.

Need AB, McKinzie JH, Mitch CH, Statnick MA, Phebus LA. In vivo rat brain opioid receptor binding of LY255582 assessed with a novel method using LC/MS/MS and the administration of three tracers simultaneously. Life Sci. 2007;81(17–18):1389–96. https://doi.org/10.1016/j.lfs.2007.09.005.

O'Brien JS, Sampson EL. Lipid composition of the normal human brain: gray matter, white matter, and myelin. J Lipid Res. 1965;6(4):537–44.

Porta Siegel T, Hamm G, Bunch J, Cappell J, Fletcher JS, Schwamborn K. Mass spectrometry imaging and integration with other imaging modalities for greater molecular understanding of biological tissues. Mol Imaging Biol. 2018;20(6):888–901. https://doi.org/10.1007/s11307-018-1267-y.

Sérrière S, Tauber C, Vercouillie J, Guilloteau D, Deloye JB, Garreau L, et al. In vivo PET quantification of the dopamine transporter in rat brain with [18F]LBT-999. Nucl Med Biol. 2014;41(1):106–13. https://doi.org/10.1016/j.nucmedbio.2013.09.007.

Shariatgorji M, Strittmatter N, Nilsson A, Källback P, Alvarsson A, Zhang X, et al. Simultaneous imaging of multiple neurotransmitters and neuroactive substances in the brain by desorption electrospray ionization mass spectrometry. Neuroimage. 2016;136:129–38. https://doi.org/10.1016/j.neuroimage.2016.05.004.

Shaw RC, Tamagnan GD, Tavares AAS. Rapidly (and Successfully) translating novel brain radiotracers from animal research into clinical use. Front Neurosci. 2020;14:871. https://doi.org/10.3389/fnins.2020.00871.

Van de Bittner GC, Ricq EL, Hooker JM. A philosophy for CNS radiotracer design. Acc Chem Res. 2014;47(10):3127–34. https://doi.org/10.1021/ar500233s.

Walch A, Rauser S, Deininger SO, Höfler H. MALDI imaging mass spectrometry for direct tissue analysis: a new frontier for molecular histology. Histochem Cell Biol. 2008;130(3):421. https://doi.org/10.1007/s00418-008-0469-9.

Westerink BHC, Damsma G, De Vries JB, Koning H. Dopamine re-uptake inhibitors show inconsistent effects on the in vivo release of dopamine as measured by intracerebral dialysis in the rat. Eur J Pharmacol. 1987;135(2):123–8. https://doi.org/10.1016/0014-2999(87)90603-0.

Wu C, Ifa DR, Manicke NE, Cooks RG. Molecular imaging of adrenal gland by desorption electrospray ionization mass spectrometry. Analyst. 2010;135(1):28–32. https://doi.org/10.1039/b919816d.

Xiao H, Sun M, Zhao R, Hong H, Zhang A, Zhang S, et al. Developing a cassette microdosing approach to enhance the throughput of PET imaging agent screening. J Pharm Biomed Anal. 2018;154:48–56. https://doi.org/10.1016/j.jpba.2018.02.063.

Publisher's Note

Springer Nature remains neutral with regard to jurisdictional claims in published maps and institutional affiliations.